IOPscience iopscience.iop.org

Home Search Collections Journals About Contact us My IOPscience

Correlated electrons and transport in a quantum point contact and in a double-quantum-dot system

This article has been downloaded from IOPscience. Please scroll down to see the full text article.

2007 J. Phys.: Condens. Matter 19 255211

(http://iopscience.iop.org/0953-8984/19/25/255211)

View the table of contents for this issue, or go to the journal homepage for more

Download details:
IP Address: 129.252.86.83
The article was downloaded on 28/05/2010 at 19:21

Please note that terms and conditions apply.

IOP PUBLISHING JOURNAL OF PHYSICS: CONDENSED MATTER

J. Phys.: Condens. Matter **19** (2007) 255211 (16pp) doi:10.1088/0953-8984/19/25/255211

Correlated electrons and transport in a quantum point contact and in a double-quantum-dot system

B R Bułka[1], T Kostyrko[2], M Ţolea[3] and I V Dinu[1,3]

[1] Institute of Molecular Physics, Polish Academy of Science, M Smoluchowskiego 17, 60-179 Poznań, Poland
[2] Institute of Physics, A Mickiewicz University, ulica Umultowska 85, 61-614 Poznań, Poland
[3] National Institute of Materials Physics, PO Box MG7, Bucharest-Magurele, Romania

E-mail: bulka@ifmpan.poznan.pl

Received 6 September 2006, in final form 7 November 2006
Published 30 May 2007
Online at stacks.iop.org/JPhysCM/19/255211

Abstract

A problem of electronic correlations is considered for two specific mesoscopic systems: the quantum point contact (QPC) and the double quantum dot (2QD) system. The systems are described using a generalized Anderson Hamiltonian. We show that charge fluctuations are relevant for electronic transport. In the QPC a local accumulation of charge and the dynamical Coulomb blockade effect lead to the 0.7 structure in the conductance characteristics. The evolution of the conductance with a magnetic field and in non-equilibrium situations is presented as well. The double quantum dot is studied in the approach, in which correlations within the 2QD are treated exactly, whereas the coupling of the 2QD to the leads is considered in the approximation valid at temperatures above the Kondo temperature. We analyse the evolution of the gate voltage dependence of the spin correlation functions and the conductance with the change of the interdot hopping. For the hopping parameter greater than a threshold value of the on-dot repulsion the physics of the device is dominated by the ground state eigenstates of the 2QD and antiferromagnetic correlations in the case of the doubly occupied 2QD. With a decrease of the interdot hopping repulsion below the threshold we observe a significant reduction of the antiferromagnetic coupling between the dots together with an enhanced occupation of the triplet states.

1. Introduction

In this paper we want to consider the influence of electronic correlations on the transport phenomena in nanostructures. Two situations are analysed: the transport through a quantum point contact (QPC) and a system of two quantum dots (2QD) connected in series. In the QPC the electronic transport depends on an electrostatic potential generated by two gate electrodes, which leads to quantization of the conductance $\mathcal{G}$. It was shown that apart from

quantized conductance steps $n \times 2e^2/h$ for integer values n, one can also observe a plateau at $0.7 \times 2e^2/h$ [1–4]. We consider a hypothesis that the 0.7 structure is due to an accumulated charge in the QPC, which changes a local potential for transmission of electronic waves through the QPC. The process is dynamical, because we assume charge fluctuations in the QPC and the transmission coefficient changes in time. It is a similar process to the Coulomb blockade and it is called the *dynamical Coulomb blockade effect*[4]. Our hypothesis is different from those known in the literature [6–9]. Many theoretical works have been focused on a spontaneous spin polarization [6] in the absence of an external magnetic field. A recent experiment [10], using a magnetic focusing technique, showed the spin polarization of QPC in the low-density regime, when $\mathcal{G} < 2e^2/h$, and the polarization is even stronger in samples with a well defined 0.7 structure. The origin of the spin polarization in a two-dimensional electron gas (2DEG) system is still mysterious. Other theoretical papers proposed an explanation based on scattering of transmitted electrons on bound singlet and triplet states formed in the QPC [7], or on electron–phonon effects [8]. Experiments performed by Cronenwett *et al* [11] showed at low temperatures a zero-bias peak in the differential conductance and the disappearance of the 0.7 structure plateau, which indicate formation of a Kondo-like correlated spin state. The role of electronic correlations in the transport was studied by Meir *et al* [9] within the Anderson model including correlated hopping. In this paper we want to consider a model in which an electronic charge can be accumulated in the QPC. Electronic correlations between the accumulated charge and flowing electrons lead to a dynamical Coulomb blockade effect, which reduces the conductance to $2/3 \times 2e^2/h$. We analyse the influence of temperature and a magnetic field on the differential conductance as well as the effects of higher source–drain voltages.

In the second part of the paper we consider the influence of accumulated electrons on the conductance through a 2QD system. Such a system is the simplest realization of a qubit, an electronic device based on coherently coupled quantum dots. Much experimental effort has been undertaken to construct a 2QD connected with the source and drain electrodes either in parallel [12] or in series [13]. The problem is more complex, because one can have two electrons and the single and triplet states have to be taken into account. A coherent coupling of these states with conducting electrons leads to the Kondo resonance [14] involving both the orbital and spin degrees of freedom of electrons [15]. The 2QD system can be considered as two Kondo impurities and described by the two impurity Anderson model [16, 17]. Depending on the relation of the inter-dot coupling to the dot–electrode coupling, one can expect two different ground states. For the strong inter-dot coupling, the ground state is antiferromagnetic (the singlet state formed by electrons at two neighbouring quantum dots), while in the opposite case, for the strong coupling between the dots and the electrodes, two Kondo singlets are formed between conducting electrons and those localized at the dots [16]. There is a competition between the two configurations, which can be controlled by the interdot coupling. Our purpose is to study the transition between these states, the role of charge fluctuations and many body excitations, and their influence on the electronic transport.

2. Correlations in quantum point contact

2.1. Description of the model and calculations of the conductance

The transmission through the QPC is controlled by the voltage applied to the gate electrodes, making an energy barrier with a slot between the Fermi sea in the source and the drain

[4] The notion of the dynamical Coulomb blockade (DCB) was used for transport in nanostructures with a fluctuating environment (also called the environmental Coulomb blockade); see [5]. In our case DCB means that flowing electrons are accumulated at the QPC for a short time and they block transmission of other electrons.

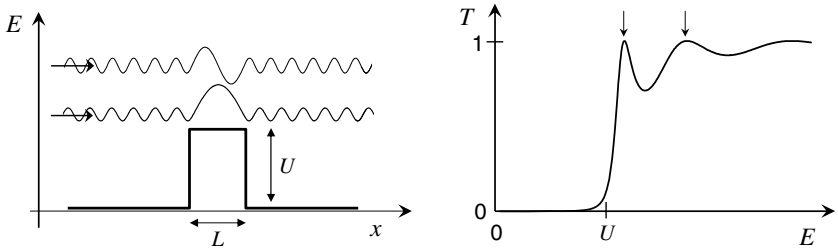

Figure 1. (Left) Schematic presentation of a potential barrier and wavefunctions corresponding to the resonant transmission. Notice a large amplitude of the wavefunction in the region of the potential barrier. (Right) The transmission coefficient T plotted as a function of the energy E of a transmitted wave. The arrows show the position of the resonant transmission.

electrodes. The real size of the slot in the experiment [11] was 0.3 μm $\times$ 0.4 μm (width $\times$ length), which is small in comparison with the Fermi wavelength $\lambda_F \approx 56$ nm in 2DEG. In a short QPC the transmission shows a series of resonant peaks—see figure 1. The first peak corresponds to the wave with the half-wavelength $\lambda_1/2$ equal to the length L of the potential barrier. The amplitude of the resonant wave and the accumulated charge are large in the region of the potential barrier. There is a ladder of resonant states, but the amplitudes of higher states are smaller and electrons prefer to occupy the lowest resonant state. The accumulated charge can lead to a reduction of the conductance if Coulomb interactions are taken into account. The process is dynamical, because an electron is captured in the QPC for a short time. The time of measurement of the current is very long with respect to the capture time, so the effective conductance depends on the average number of accumulated electrons. We call this process the dynamical Coulomb blockade [5]. The capture time in this case is much longer than the relaxation time and the current is reduced to zero at low temperatures.

We want to prove that the conductance is reduced to the value $2/3 \times 2e^2/h$ due to the dynamical Coulomb blockade effect. Our studies focus on the lowest resonant state ϵ_0 and the higher states are treated as a continuum energy sub-band. An electron transmitted through the resonant state interacts with the accumulated charge, but the transmission via the sub-band states is like that for free electrons with the perfect transmission corresponding to the $2e^2/h$ plateau in the conductance. The model can be described by an extended single-level Anderson Hamiltonian

$$H = \sum_{k,\sigma,\alpha\in L,R} \epsilon_{k\alpha}\, c^{\dagger}_{k\alpha,\sigma} c_{k\alpha,\sigma} + \sum_{\sigma}\left(\epsilon_0\, d^{\dagger}_{0\sigma} d_{0\sigma} + \frac{U}{2}\, n_{0\sigma} n_{0-\sigma}\right) + \sum_{k,\sigma,\alpha\in L,R} (t_\alpha\, c^{\dagger}_{k\alpha,\sigma} d_{0\sigma} + \text{h.c.}) + \sum_{k,\sigma} (t_{kLR}\, c^{\dagger}_{kL,\sigma} c_{kR,\sigma} + \text{h.c.}). \tag{1}$$

The first term describes electrons in the left ($\alpha = L$) and the right ($\alpha = R$) electrode; the second one corresponds to an electron in the resonant state ϵ_0 and the Coulomb interaction of two electrons with opposite spins; the third one describes tunnelling of electrons from the electrodes through the resonant state; and the last one corresponds the direct transmission of electronic waves via the sub-band states.

The current (from the left electrode) is calculated by means of the non-equilibrium Green functions [18]

$$I = -e\left\langle \frac{\mathrm{d}}{\mathrm{d}t} \sum_{k,\sigma} n_{kL\sigma} \right\rangle = \frac{2e}{\hbar} \int \frac{\mathrm{d}E}{2\pi} \mathrm{Re}\Big[\sum_{k,\sigma} t_L\; G^{<}_{0,kL\sigma}(E) + \sum_{k,\sigma} t_{kLR}\; G^{<}_{kR\sigma,kL\sigma}(E)\Big], \tag{2}$$

where $G^{<}_{0,kL\sigma}$ is the lesser Green function corresponding to the resonant state and the state in the left electrode and $G^{<}_{kR\sigma,kL\sigma}$ the lesser Green function between the states in both the electrodes. Using the Dyson equation we calculate the non-equilibrium Green functions and express J only by the local Green function G_{00} and the bare Green functions in the electrodes: $g^{<}_{\alpha} = 2\mathrm{i}\pi\rho f_\alpha$ and $g^{r,a}_{\alpha} = \mp\mathrm{i}\pi\rho$. Here, f_α denotes the Fermi distribution function in the α-electrode, in which the chemical potential is μ_α. Our calculations are performed for a symmetrically applied source–drain voltage V_{sd}, i.e. $\mu_L = E_{\mathrm{F}} + eV_{\mathrm{sd}}/2$ and $\mu_R = E_{\mathrm{F}} - eV_{\mathrm{sd}}/2$ with respect to the Fermi energy E_{F}. We also assume the constant density of states $\rho(E) = 1/2D$ for $|E| < D$ and D is taken as unity in the further calculations. In the case of quasi-elastic transport, for which the current conservation rule is fulfilled for any energy E, one can determine the local Wigner distribution function and can obtain an exact formula for the current

$$I = \frac{e}{h}\int \mathrm{d}E\,[f_L(E) - f_R(E)]\sum_{\sigma}\{\alpha_{LR}(E) + \mathrm{Im}[\alpha_{00}(E)G^{r}_{0\sigma,0\sigma}(E)]\}, \tag{3}$$

where $\alpha_{LR}(E) = 4\pi^2\rho^2 t^2_{LR}/w^2$, $\alpha_{00}(E) = -4\pi\rho z^2_L z^2_R/[w^2(|z_L|^2 + |z_R|^2)]$, $w(E) = 1 + \pi^2\rho^2 t^2_{LR}$, $z_L = t_L - \mathrm{i}\pi\rho t_{LR}t_R$, $z_R = t_R - \mathrm{i}\pi\rho t_{LR}t_L$. We assume that the coefficient $t_{LR}(E)$ depends on E of a transmitted wave and it is expressed as $t_{LR}(E) = t^0_{LR}/\{1 + \exp[-(E - h_{\mathrm{b}})/s_{LR}]\}$. Here, h_{b} denotes a separation of the sub-band from the resonant state; s_{LR} is a slope of the curve. To ensure the perfect transmission for energies in the sub-band region we chose $t^0_{LR} = 1/(\pi\rho)$. We have checked that the functional form of $t_{LR}(E)$ has a minor quantitative effect on the results presented.

In order to determine the Green function $G^{r}_{0\uparrow,0\uparrow}$ we use the equation of motion (EOM) method

$$(E - \epsilon_0)G^{r}_{0\uparrow,0\uparrow} = 1 + \sum_{k,\alpha} t_\alpha G^{r}_{k\alpha\uparrow,0\uparrow} + U G^{r}_{0\uparrow 0\downarrow 0\downarrow,0\uparrow}. \tag{4}$$

The equation involves a higher order Green function $G^{r}_{0\uparrow 0\downarrow 0\downarrow,0\uparrow} = \langle\langle d_{0\uparrow}d^{\dagger}_{0\downarrow}d_{0\downarrow}|d^{\dagger}_{0\uparrow}\rangle\rangle^{r}$, for which one can write the equation of motion

$$(E - \epsilon_0 - U)G^{r}_{0\uparrow 0\downarrow 0\downarrow,0\uparrow} = \langle n_{0\downarrow}\rangle + \sum_{k,\alpha} t_\alpha (G^{r}_{k\alpha\uparrow 0\downarrow 0\downarrow,0\uparrow} - G^{r}_{0\uparrow k\alpha\downarrow 0\downarrow,0\uparrow} + G^{r}_{0\uparrow 0\downarrow k\alpha\downarrow,0\uparrow}) \tag{5}$$

where $\langle n_{0\downarrow}\rangle$ is an average number of electrons with spin $\downarrow$ accumulated at the resonant state. The Green functions $G^{r}_{k\alpha\uparrow 0\downarrow 0\downarrow,0\uparrow} = \langle\langle c_{k\alpha\uparrow}d^{\dagger}_{0\downarrow}d_{0\downarrow}|d^{\dagger}_{0\uparrow}\rangle\rangle^{r}$, $G^{r}_{0\uparrow k\alpha\downarrow 0\downarrow,0\uparrow} = \langle\langle d_{0\uparrow}c^{\dagger}_{k\alpha\downarrow}d_{0\downarrow}|d^{\dagger}_{0\uparrow}\rangle\rangle^{r}$ and $G^{r}_{0\uparrow 0\downarrow k\alpha\downarrow,0\uparrow} = \langle\langle d_{0\uparrow}d^{\dagger}_{0\downarrow}c_{k\alpha\downarrow}|d^{\dagger}_{0\uparrow}\rangle\rangle^{r}$ describe the coupling of electrons at the QPC with the electrodes and they are treated in an approximate way

$$\sum_k t_\alpha G^{r}_{k\alpha\uparrow 0\downarrow 0\downarrow,0\uparrow} \approx \sum_k t_\alpha G^{r}_{0\uparrow k\alpha\downarrow 0\downarrow,0\uparrow} \approx \sum_k t_\alpha G^{r}_{0\uparrow 0\downarrow k\alpha\downarrow,0\uparrow} \approx -\mathrm{i}\pi t^2_\alpha\rho\; G^{r}_{0\uparrow 0\downarrow 0\downarrow,0\uparrow}. \tag{6}$$

This approximation is perturbative to the order of t^2_α. (A similar approximation was used in [19], which for a single quantum dot gives the results of Meir *et al* [20]—the same decoupling is used in the section 3.1.) Charge fluctuations are included, but spin-flip processes, which lead to the Kondo resonance, are neglected. It corresponds to a high temperature regime (for temperatures higher than the Kondo temperature T_{K}), when the Abrikosov–Suhl peak in the density of states is absent. In the limit $U \to \infty$ the calculations are simpler and one gets $UG^{r}_{0\uparrow 0\downarrow 0\downarrow,0\uparrow} \approx -\langle n_{0\downarrow}\rangle$. Thus, from equation (4)

$$G^{r}_{0\uparrow,0\uparrow}(E) = \frac{1 - \langle n_{0\downarrow}\rangle}{E - \epsilon_0 + \mathrm{i}\Delta_0}, \tag{7}$$

where $\Delta_0 = \pi\rho(t^2_L + t^2_R)$. The electron concentration is expressed as

$$\langle n_{0\uparrow}\rangle = -\frac{1}{\pi}\int \mathrm{d}\omega\; f_0(E)\mathrm{Im}[G^{r}_{0\uparrow,0\uparrow}(E)], \tag{8}$$

where $f_0(E) = \gamma_L f_L(E) + \gamma_R f_R(E)$ is the Wigner distribution function at the resonant state, $\gamma_L = |z_L|^2/(|z_L|^2 + |z_R|^2)$ and $\gamma_R = |z_R|^2/(|z_L|^2 + |z_R|^2)$.

2.2. Analysis of the conductance in the quantum point contact

Now, we want to analyse the electronic transport through the QPC, which can be calculated numerically from equations (3) and (7)–(8). However, we first present a simplified analysis. The electron concentration is calculated in a self-consistent way and in the zero-bias limit one gets from equation (8) $\langle n_{0\uparrow}\rangle = (1 - \langle n_{0\downarrow}\rangle)X$, where $X = (1/\pi)\int \mathrm{d}E\, f_0(E)\Delta_0/[(E - \epsilon_0)^2 + \Delta_0^2]$. If the Fermi level is close to the resonant transmission ($E_\mathrm{F} \approx \epsilon_0$), one gets $X \approx 1/2$, and a paramagnetic solution $\langle n_{0\uparrow}\rangle = \langle n_{0\downarrow}\rangle \approx 1/3$. In this simplified analysis we neglect the interference effect between the resonant and the direct channel, which can occur in a small range of the gate voltage and is smeared by temperature. For the resonant transmission the first term in equation (3) is irrelevant, and the second term leads to the conductance $\mathcal{G}_0 = \mathrm{d}I/\mathrm{d}V_\mathrm{sd}|_{V_\mathrm{sd}=0}$ proportional to $\mathrm{Im}[G^r_{0\uparrow,0\uparrow}(E_\mathrm{F})]$. Therefore, the conductance has a first plateau at $\mathcal{G} \approx (1 - \langle n_{0\downarrow}\rangle) \times 2e^2/h \approx 2/3 \times 2e^2/h$. The second plateau is at $2e^2/h$, when the Fermi level goes above the potential barriers ($E_\mathrm{F} > h_\mathrm{b}$) and the transport is ballistic.

We have shown that the position of the first 'anomalous' conductance plateau is related to the accumulation of charge. Due to the dynamical Coulomb effect the conductance is not perfect, but reduced by a factor $(1 - \langle n_{0-\sigma}\rangle)$, which for the resonant transmission is equal to two-thirds. In the non-equilibrium situation, the electronic occupancy can have various values, leading to new positions of the plateau, and the picture is more complicated, as we describe below.

For a non-equilibrium situation (for large V_sd) one can distinguish three cases: (i) when the Fermi energy E_F is close to the edge of the 2/3 plateau, (ii) E_F is close to h_b (deep in the 2/3 plateau and close to the 1 plateau) and (iii) in the range of the 1 plateau for $E_\mathrm{F} > h_\mathrm{b}$. For case (i) the applied potential V_sd shifts μ_R below the resonant energy range ($\mu_R \ll V_\mathrm{sd}$), while the chemical potential in the left electrode can be still in the resonant regime $\mu_L \approx \epsilon_0$. Using the relation for the Wigner distribution function $f_0(E) = \gamma_L f_L(E) + \gamma_R f_R(E)$ we can express the integral $X = X_L + X_R$ as two contributions from the left and the right electrode. For this case $X_L \approx 1/4$, $X_R \approx 0$ and $X \approx 1/4$, which yields $\langle n_{0\uparrow}\rangle \approx 1/5$. The differential conductance $\mathcal{G} = \mathrm{d}I/\mathrm{d}V_\mathrm{sd}$ also includes two contributions $\mathcal{G}_L$ and $\mathcal{G}_R$. In the considered case $\mathcal{G}_R = 0$ and therefore $\mathcal{G} = \mathcal{G}_L \approx 2/5 \times 2e^2/h$. In case (ii) the chemical potential μ_L can be shifted above the tunnel barrier ($\mu_L > h_\mathrm{b}$), while $\mu_R \approx \epsilon_0$. Both channels, the ballistic and the resonant one, contribute to the transport. In this case $X_L \approx 1/2$, $X_R \approx 1/4$, $X \approx 3/4$ and $\langle n_{0\uparrow}\rangle \approx 3/7$. The ballistic channel gives $\mathcal{G}_L \approx 1/2 \times 2e^2/h$ and the resonant transmission $\mathcal{G}_R \approx 2/7 \times 2e^2/h$. It means that with increasing V_sd the differential conductance increases from $2/3 \times 2e^2/h$ and reaches its maximal value $11/14 \times 2e^2/h \approx 0.79 \times 2e^2/h$ for large voltages. In case (iii) $E_\mathrm{F} > h_\mathrm{b}$, the ballistic channel only participates in the transport and $\mathcal{G}$ is kept at $2e^2/h$ if the voltage is small, $eV_\mathrm{sd}/2 < (E_\mathrm{F} - h_\mathrm{b})$. However, for larger V_sd the resonant channel becomes activated and the conductance drops to $\mathcal{G} \approx 0.79 \times 2e^2/h$.

The results of self-consistent numerical calculations of the electron concentration from equations (7)–(8) and the conductance from equation (3) are presented in figures 2 and 3. As one can expect, the conductance steps are smeared for $k_\mathrm{B}T \approx \Delta_0$, which is also presented in figure 2(a). The applied magnetic field B shifts the energy levels $\Delta E = \pm g\mu_\mathrm{B}B$ for spin $\sigma = \uparrow$ and $\downarrow$. It changes the occupation numbers $\langle n_{0\uparrow}\rangle$ and $\langle n_{0\downarrow}\rangle$ as well as the conductance $\mathcal{G}$ (see figure 2(b)). Figure 3 shows the set of differential conductance curves in the absence of the magnetic field ($B = 0$) and in magnetic field ($g\mu_\mathrm{B}B = 0.06$ in units of the bandwidth D). The figures confirm the previous analysis and show the evolution of the conductance curves

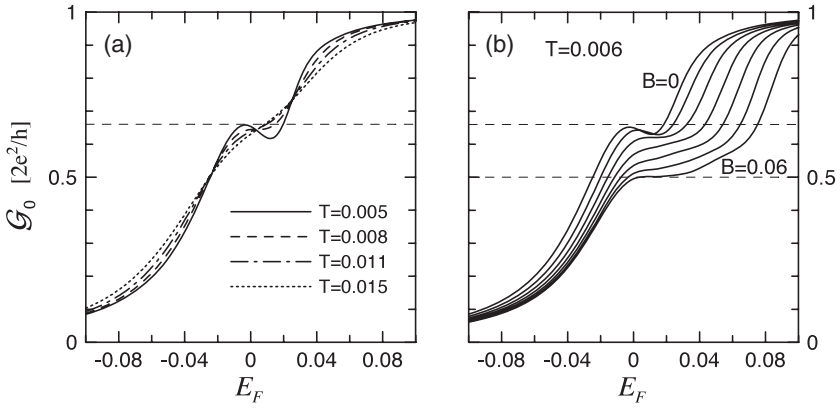

Figure 2. The conductance $\mathcal{G}_0 = \mathrm{d}I/\mathrm{d}V_{\mathrm{sd}}|_{V_{\mathrm{sd}}=0}$ as a function of the Fermi level E_{F} for different temperatures (a) and for different magnetic fields $0 \leqslant g\mu_{\mathrm{B}}B \leqslant 0.06$ at $k_{\mathrm{B}}T = 0.006$ (b). The half-bandwidth D of the electronic band in the electrodes is taken as unity, the coupling $t_L = t_R = 0.1$, $\Delta_0 = 0.0314$, the direct inter-electrode hopping $t_{LR} = t^0_{LR}/\{1 + \exp[-(E - h_{\mathrm{b}})/s_{LR}]\}$, $t^0_{LR} = 2D/\pi$, $h_{\mathrm{b}} = 0.025$, $s_{LR} = 0.003$.

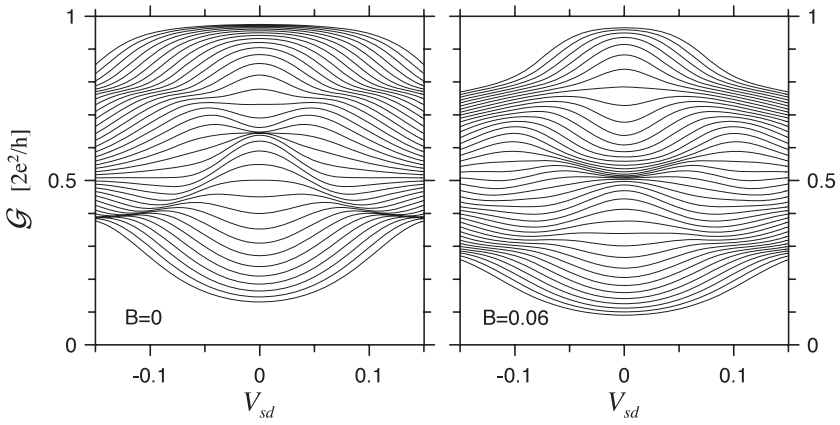

Figure 3. The differential conductance $\mathcal{G} = \mathrm{d}I/\mathrm{d}V_{\mathrm{sd}}$ as a function of the source–drain voltage V_{sd} for $-0.08 \leqslant E_{\mathrm{F}} \leqslant 0.10$ (from bottom to top curve) at $k_{\mathrm{B}}T = 0.006$ for a magnetic field $B = 0$ and $g\mu_{\mathrm{B}}B = 0.06$. The other parameters are the same as in figure 2.

with increasing V_{sd}. The conductance from the value $\mathcal{G} = 2e^2/h$ drops to c.a. $0.8 \times 2e^2/h$. If $\mathcal{G} = 2/3 \times 2e^2/h$ at V_{sd} then it evolves either to $0.8 \times 2e^2/h$ or to $0.4 \times 2e^2/h$. The lower conductance curves (corresponding $E_{\mathrm{F}} < \epsilon_0$) increase, reach a maximum and drop to $0.4 \times 2e^2/h$. When the magnetic field is applied (figure 3(b)) the conductance curves are similar to those in figure 3(a), with a pronounced plateau at $0.5 \times 2e^2/h$.

Let us compare the plots in figure 3 with the experimental data in [11, 4]. The experimental and the theoretical plots are similar in the high conductance region. The experimental plots show the evolution of $\mathcal{G}$ from $2e^2/h$ and $0.7 \times 2e^2/h$ to $0.8 \times 2e^2/h$—similarly to the curves in figure 3. In the lower conductance range the theoretical curves are different from those in experiment. In high V_{sd} the experimental plots merge at $0.25 \times 2e^2/h$ [11], and at 0.25–$0.4 \times 2e^2/h$ [4]. The experiments show that the source–drain voltage V_{sd} has a strong influence on the electronic transport. The differential conductance curves change significantly

in the range of a few millivolts, especially those with low conductance. This suggests a modification of the potential barrier in the QPC with an increase in $V_{\rm sd}$, which has a strong influence on the conductance. In the present model we assumed only a shift of the chemical potentials μ_α in the electrodes with $V_{\rm sd}$. The energy structure of QPC (the position of the resonant level ϵ_0 and the coefficients t_α) was taken as independent of $V_{\rm sd}$.

3. Double-quantum-dot system correlations

3.1. Presentation of the model and the Hubbard operator method

Our 2QD system will be described by the two-impurity Anderson model, which will be studied by means of the EOM approach taking into account charge fluctuations. The EOM with various approximate decoupling procedures for the higher order Green functions was used in the literature [22, 23]. The disadvantage of these procedures lies in omitting higher order correlation functions and neglecting a contribution to transport from transmission channels through excited states. In the present paper we apply the Hubbard operators [24] and the decoupling procedure, which treats all electronic correlations exactly within the 2QD system and requires determination of various intra- and interdot correlation functions, which are computed here in a fully self-consistent way. In our decoupling some higher order correlations between electrons at the 2QD and conducting electrons from the electrodes are omitted, which is justified above the temperatures typical of the Kondo effect.

The Hamiltonian for two quantum dots connected in series is given by

$$\begin{aligned} H = H_{\rm el} + H_{\rm 2QD} + H_{\rm el-2QD} = & \sum_{k,\alpha,\sigma} \epsilon_{k\alpha}\, c^\dagger_{k\alpha,\sigma} c_{k\alpha,\sigma} \\ & + \sum_{i,\sigma} \epsilon_i\, d^\dagger_{i\sigma} d_{i\sigma} + t \sum_{\sigma} (d^\dagger_{1,\sigma} d_{2,\sigma} + d^\dagger_{2,\sigma} d_{1,\sigma}) + \frac{U}{2} \sum_{i,\sigma}\, n_{i,\sigma}\, n_{i,-\sigma} \\ & + t_L \sum_{k,\sigma} (c^\dagger_{kL,\sigma} d_{1,\sigma} + \text{h.c.}) + t_R \sum_{k,\sigma} (c^\dagger_{kR,\sigma} d_{2,\sigma} + \text{h.c.}), \end{aligned} \tag{9}$$

where the first term describes electrons in the electrodes ($\alpha = L, R$); the second, third and fourth terms correspond to electrons at 2QD with a local electron potential energy $\epsilon_{i\sigma}$, an electron transfer t between the quantum dots and intradot Coulomb interactions U; the coupling of 2QD to the electrodes is described by two last terms. We rewrite the 2QD Hamiltonian using Hubbard operators [24]

$$H_{\rm 2QD} = \sum_{\lambda} E_\lambda X_{\lambda\lambda}. \tag{10}$$

Above, E_λ denotes the exact eigenvalue of 2QD in the external potential generated by the leads. The Hubbard operators are represented in terms of the exact eigenstates of the 2QD Hamiltonian, $|\mu\rangle, |\nu\rangle$ as $X_{\mu\nu} = |\mu\rangle\langle\nu|$. An arbitrary electron operator referring to the dimer degrees of freedom can be expanded as a linear combination of the Hubbard operators

$$\mathcal{O} = \sum_{\lambda\lambda'} \langle\lambda|\mathcal{O}|\lambda'\rangle\, X_{\lambda\lambda'}. \tag{11}$$

Using equation (11) the one-particle Green functions can be written in terms of linear combinations of the mixed Green functions, defined with the help of Hubbard operators and the single-particle operators

$$G_{j\sigma,m\sigma} = \sum_{\lambda\lambda'} p^{\lambda\lambda'}_{j\sigma}\, G_{\lambda\lambda',m\sigma}, \qquad p^{\lambda\lambda'}_{j\sigma} = \langle\lambda|d_{j\sigma}|\lambda'\rangle, \tag{12}$$

where $G_{\lambda\lambda',m\sigma} = \langle\langle X_{\lambda\lambda'}|d^\dagger_{m\sigma}\rangle\rangle$. The equations of motion for $G_{\lambda\lambda',m\sigma}$ generate a chain of higher order Green functions. This can be written schematically as

$$\frac{\mathrm{d}}{\mathrm{d}t}\langle\langle X^F|d^\dagger_{m\sigma}\rangle\rangle \to \langle\langle X^{B0(B2)}c^{(\dagger)}_{k\alpha\sigma'}|d^\dagger_{m\sigma}\rangle\rangle, \tag{13}$$

$$\frac{\mathrm{d}}{\mathrm{d}t}\langle\langle X^{B0}c_{k\alpha\sigma'}|d^\dagger_{m\sigma}\rangle\rangle \to \langle\langle X^F c^\dagger_{k'\alpha'\sigma''}c_{k\alpha\sigma'}|d^\dagger_{m\sigma}\rangle\rangle, \tag{14}$$

where Bn indicates a boson-like Hubbard operator which reduces the number of electrons in a state by n and F denotes a fermion-like Hubbard operator, removing a single electron from a state. In order to close the set of equations we neglect electron correlations between the 2QD and the leads and decouple the higher order Green function from equation (14) as follows:

$$\langle\langle X^F_{\zeta\zeta'}c^\dagger_{k'\alpha'\sigma''}c_{k\alpha\sigma'}|d^\dagger_{m\sigma}\rangle\rangle \to \delta_{k'\alpha'\sigma'',k\alpha\sigma'}\, f_\alpha\, \langle\langle X^F_{\zeta\zeta'}|d^\dagger_{m\sigma}\rangle\rangle \tag{15}$$

where f_α is the Fermi function for the α lead. For a single quantum dot this approximation reduces to the results of Meir *et al* [20] and correctly describes the limit of the Coulomb blockade. In the non-interacting limit of the Hubbard model it reproduces the exact results. For the finite repulsion U the neglect of the lead–2QD correlations is credible for temperatures higher than the Kondo temperature. In our numerical computation we evaluated the poles of the Green functions in the high temperature approximation (we set $f_\alpha = 1/2$), neglecting the Kondo divergences. Alternatively, we can decouple the retarded and the advanced Green functions as

$$\langle\langle c_{k\alpha\sigma'}X|d^\dagger_{m\sigma}\rangle\rangle^{r,a} \approx \tfrac{1}{2}\,t_\alpha\, g^{r,a}_\alpha\, \langle\langle\{d_{\alpha\sigma'}, X\}\,|d^\dagger_{m\sigma}\rangle\rangle^{r,a}, \tag{16}$$

which leads to the same result for the Green functions as the high temperature approximation for equation (15).

The lesser Green functions are obtained according to the EOM procedure described by Niu *et al* [25]. For the corresponding decoupling of the Green function we assume that, by an analogy with equation (16),

$$\langle\langle c^\dagger_{k\alpha\sigma'}X|d^\dagger_{m\sigma}\rangle\rangle^{<} \approx \tfrac{1}{2}\,t_\alpha\, g^r_\alpha\, \langle\langle\{d_{\alpha\sigma'}, X\}\,|d^\dagger_{m\sigma}\rangle\rangle^{<} + \tfrac{1}{2}\,t_\alpha\, g^<_\alpha\, \langle\langle\{d_{\alpha\sigma'}, X\}\,|d^\dagger_{m\sigma}\rangle\rangle^{a}. \tag{17}$$

Using equation (16)–(17) one can obtain the explicit results for the energy Fourier transforms of the retarded, advanced and lesser Green functions. They can be obtained in terms of the exact eigenvalues of the dimer Hamiltonian, equation (10), the matrix elements of the electron operators between the eigenstates of $H_{2\mathrm{QD}}$, and the averages of the boson–like Hubbard operators [21]. In general, they are linear combinations of terms of the form $R_{\mu\nu}\left(E - E_\mu + E_\nu + Q_{\mu\nu}\right)^{-1}$. Here, $Q_{\mu\nu}$ is a line broadening term, depending on the matrix elements of the electron operators and the coupling to the leads, $R_{\mu\nu}$ is the residuum including products of the matrix elements and the averages of the Hubbard operators and E is the energy. The approximations defined by equations (16)–(17) reduce to the exact result in the limiting cases of Coulomb blockade as well as the noninteracting limit and in between they serve as the interpolating ansatz. In this approach all the intradimer charge and spin correlations are taken into account accurately. On the other hand the coupling with the electrodes is treated perturbatively to the second order t^2_α, in which the charge fluctuations are taken into account, but the Kondo type effects (depending on higher order correlations with electrons from the leads) are neglected. The residua of the advanced and the retarded Green functions are determined by the averages of the bosonic Hubbard operators. These averages are self-consistently computed using the lesser Green functions,

$$\langle X^B_{\gamma\lambda'}\rangle = \frac{1}{N_\gamma}\sum_{\lambda\sigma m}\langle\lambda|d^\dagger_{m\sigma}|\gamma\rangle \int \frac{\mathrm{d}E}{2\pi\mathrm{i}}\, G^<_{\lambda\lambda',m\sigma}(E). \tag{18}$$

Since the poles of the Green functions do not depend on $\langle X^B_{\gamma\lambda'}\rangle$, the system of the equations used to determine the averages is a linear one. From the averages of the boson–like Hubbard operators, and using equation (11), arbitrary intradimer spin and charge correlation functions can be easily found, e.g.

$$\langle n_{1\sigma}n_{2\sigma'}\rangle = \sum_{\lambda,\lambda'}\langle\lambda'|n_{1\sigma}n_{2\sigma'}|\lambda\rangle\langle X^B_{\lambda\lambda'}\rangle \tag{19}$$

and the spin–spin correlation function reads

$$\langle \mathbf{S}_1\cdot\mathbf{S}_2\rangle = -\tfrac{3}{4}\sum_{\sigma\sigma'}(-1)^{\delta_{\sigma\sigma'}}\langle n_{1\sigma}n_{2\sigma'}\rangle. \tag{20}$$

In order to determine the current we start from a general formula of Meir and Wingreen [20]

$$I = \frac{\mathrm{i}e}{h}\int \mathrm{d}\omega\,\Gamma_L\sum_{\sigma}\left\{f_L(E)\left[G^r_{1\sigma,1\sigma}(E) - G^a_{1\sigma,1\sigma}(E)\right] + G^<_{1\sigma,1\sigma}(E)\right\}, \tag{21}$$

where $\Gamma_\alpha = 2\pi\rho t_\alpha^2$. Inserting the results for the Green function into the integral (21) one finally obtains an explicit result for the current in the form [21]

$$I = \frac{2e\Gamma_L\Gamma_R}{h}\sum_{\lambda\lambda'\mu\mu'}\frac{1}{2}\left(p^{\lambda\lambda'}_{L\sigma}\left\langle\left\{d^\dagger_{L\sigma}, X^F_{\mu\mu'}\right\}\right\rangle + p^{*\mu\mu'}_{L\sigma}\left\langle\left\{d^\dagger_{L\sigma}, X^F_{\lambda\lambda'}\right\}\right\rangle^*\right)$$
$$\times\int \mathrm{d}E\,(f_L - f_R)\left[\left(E\hat{1} - \hat{\Omega} - \hat{Q}^r\right)^{-1} q_R\left(E\hat{1} - \hat{\Omega} - \hat{Q}^a\right)^{-1}\right]_{\lambda\lambda',\mu\mu'}, \tag{22}$$

where $\hat{\Omega}_{\lambda\lambda',\mu\mu'} = \delta_{\lambda\lambda',\mu\mu'}\,(E_\lambda - E_{\lambda'})$, $\hat{Q}^r = -\mathrm{i}\sum_\alpha\Gamma_\alpha q_\alpha$, $\hat{Q}^r = -\hat{Q}^a$, and $(q_\alpha)_{\nu\nu',\zeta\zeta'} = \delta_{\nu\nu',\zeta\zeta'} + \frac{1}{2}\sum_{\sigma,\alpha}(p^{\nu\zeta}_{\alpha\sigma}\,p^{\nu'\zeta'}_{\alpha\sigma} + p^{\zeta\nu}_{\alpha\sigma}\,p^{\zeta'\nu'}_{\alpha\sigma})$.

3.2. Analysis of correlation functions and transport in double quantum dot system

Now, we can calculate all correlation functions and the conductance in the 2QD system by means of the procedure described above. We want to study many electron configurations depending on the parameters of the model and their influence on the electronic transport. Our attention is focused on a spin configuration, which can be changed with the interdot coupling. Two limiting cases are interesting: (i) for the strong interdot coupling (stronger than the coupling to the electrodes, $t \gg \Gamma$) and (ii) the strong coupling of 2QD to the electrodes ($\Gamma \gg t$). In case (i) two electrons occupy the singlet ground state, while in case (ii) the spins localized at the dots are decoupled.

The parameters of the 2QD system can be tuned in the experiment by gate voltages—one can change the energy level position ϵ_i, the hybridization between the dots t and the coupling to the electrodes Γ_α. Figure 4 presents the correlation functions plotted versus the position of the energy level in the dots $E = \epsilon_1 = \epsilon_2$. We assume that the Fermi energy $E_\mathrm{F} = 0$ and the levels in both dots are simultaneously shifted by the gate voltage. It is seen that the electron concentration $\langle n_{1\uparrow}\rangle$ (dotted curve) increases with decreasing E. The thin vertical lines show the regions in which the 2QD system has one, two and three electrons. These lines also indicate the position of the levels for resonant transmission. The length of the total spin $\langle \mathbf{S}^2_\mathrm{tot}\rangle$ (solid curve) is about 0.75 in the one electron (hole) region—in this case one free spin is in the system. In the centre of the plot, corresponding to two electrons present at the 2QD, the value of $\langle \mathbf{S}^2_\mathrm{tot}\rangle$ depends on the interdot coupling t—compare figures 4(a) and (b) for $t = 1$ and 0.25, respectively. For large t, the length of the total spin is strongly reduced and achieves its minimal value $\langle \mathbf{S}^2_\mathrm{tot}\rangle = 0.03$. The 2QD system is then in the molecular state and both the spins are strongly coupled. The spin–spin correlator $\langle \mathbf{S}_1\cdot\mathbf{S}_2\rangle$ (dashed curve) is negative and its absolute value increases with the second electron entering the 2QD (see figure 4(a)).

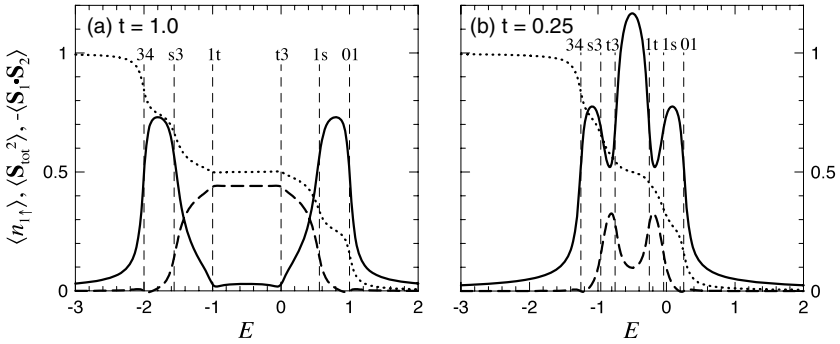

Figure 4. The average number of electrons $\langle n_{1\uparrow}\rangle$ per spin at the quantum dot (dotted curve), the square of the total spin length $\langle \mathbf{S}_{\rm tot}^2\rangle$ (solid curve), the spin–spin correlator $-\langle \mathbf{S}_1 \cdot \mathbf{S}_2\rangle$ (dashed curve) plotted as a function of the energy level $\epsilon_1 = \epsilon_2 = E$ for the hopping integral $t = 1$ (a) and $t = 0.25$ (b) at $U = 1$, with the electrode–2QD coupling $\Gamma = 0.05$, the Fermi energy $E_{\rm F} = 0$ and the temperature $T = 0$. The vertical dashed lines denoted '01' and '34' indicate the positions of the resonant levels at $\Delta E_{01} = E_0 - E_1$ and $\Delta E_{34} = E_3 - E_4$, which correspond to the charge fluctuations from the zero-electron state to the one-electron state and from the three-electron state to the four-electron state, respectively. Similarly, the dashed lines denoted '1s', '1t' or 's3', 't3' indicate the resonant transmissions at the energies $\Delta E_{1\rm s} = E_1 - E_-$, $\Delta E_{1\rm t} = E_1 - E_t$, or $\Delta E_{s3} = E_- - E_3$, $\Delta E_{t3} = E_{\rm t} - E_3$ (they correspond to the charge fluctuations either from the one-electron ground or from the three-electron ground state to the singlet state, to the triplet state).

Figure 4(b) presents the plots for the weak interdot coupling $t = 0.25$. The plots are different from those in figure 4(a). At the centre of the figure $\langle \mathbf{S}_{\rm tot}^2\rangle$ reaches its maximal value 1.16, which is not so far from the value 1.5 for the length of the total spin of two free electrons. It means that the spins are weakly coupled. This statement confirms the plot of the spin–spin correlation function $-\langle \mathbf{S}_1 \cdot \mathbf{S}_2\rangle$, which shows a pronounced minimum in the centre of the figure. The plot of $-\langle \mathbf{S}_1 \cdot \mathbf{S}_2\rangle$ shows an increase in the antiferromagnetic coupling when the singlet state becomes occupied. However, the spin–spin correlation function drops when the triplet state starts to participate in the transport.

Figure 5 shows the dependence of the spin correlation functions on the interdot coupling parameter t in the centre of the electronic structure ($E = U/2$). In the atomic limit (for small t) there are two uncoupled spins. The square of the spin length $\langle \mathbf{S}_1^2\rangle$ localized at each quantum dot is a little bit smaller than three-quarters for the square of the spin length of a free electron. The reduction is due to the electrode–2QD charge fluctuations, and the effect is more pronounced for a larger Γ_α. The value of $\langle \mathbf{S}_1^2\rangle$ monotonically decreases with increasing t. The spin–spin correlation function $-\langle \mathbf{S}_1 \cdot \mathbf{S}_2\rangle$ increases in the first stage, reaches a maximum and decreases for large t. The interdot spin coupling in the Hubbard dimer is given by $J \approx 4t^2/U$ for a large t. The charge fluctuations lead to the reduction of $-\langle \mathbf{S}_1 \cdot \mathbf{S}_2\rangle$, which is more pronounced in the region where $J \ll \Gamma_\alpha$. In order to show the role of charge fluctuations we calculated the spin correlation functions for an ensemble of the dimers, coupled with a thermal reservoir (see the appendix for details of the calculations). One can expect an increase of charge fluctuations with increasing temperature T. The results, presented by the thin curves in figure 5, are qualitatively close to those for the 2QD system. They confirm our hypothesis on the role of charge fluctuations. The transition from the molecular state (with strongly coupled spins) to the atomic state (with decoupled spins) depends on charge fluctuations and participation of the triplet state. If the charge fluctuations are strong, an electron from the singlet state can be easily transferred to the reservoir and next to the triplet state. This is an incoherent process, which reduces the effective interdot spin coupling.

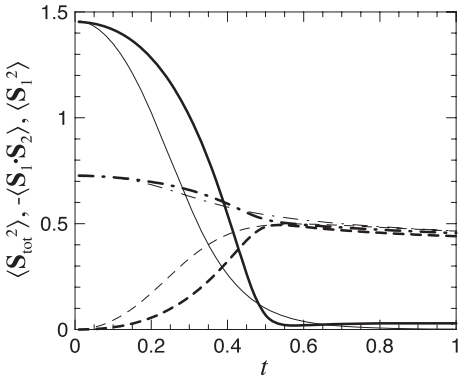

Figure 5. The correlation functions: $\langle \mathbf{S}_{\rm tot}^2 \rangle$ (solid curve), $-\langle \mathbf{S}_1 \cdot \mathbf{S}_2 \rangle$ (dashed curve) and $\langle \mathbf{S}_1^2 \rangle$ (dot–dash curve) as a function of the interdot hopping integral t at the centre of electronic structure (at $E = U/2$) and for $U = 1$, $\Gamma = 0.05$, $T = 0$. The thin curves correspond to the correlation functions calculated for an ensemble of dimers (presented in the appendix) at the temperature $T = 0.14$, at which $\langle \mathbf{S}_{\rm tot}^2 \rangle$ has the same value as in the 2QD system for $t = 0.01$.

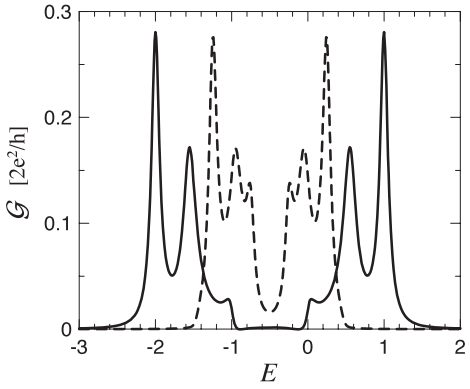

Figure 6. The conductance as a function of the energy level $\epsilon_1 = \epsilon_2 = E$ for the hopping integral $t = 1$ (solid curve) and $t = 0.25$ (dashed curve) at $U = 1$, the electrode–2QD coupling $\Gamma = 0.05$ and the Fermi energy $E_{\rm F} = 0$. The peaks (from the right-hand side) correspond to the resonant states: for the one electron, for the singlet and for the triplet; and symmetrically (from the left-hand side) for the one hole, for the singlet and for the triplet.

The conductance calculated by means of the Hubbard operators is presented in figure 6. Usually one gets four peak conductance characteristics in the 2QD system (see e.g. [22, 23]), in which the peaks correspond to the resonant transmission through the ground states. Our procedure takes into account all many electron states and the corresponding poles in the Green functions $(E_\lambda - E_{\lambda'})$—see equation (22). Figure 6 also shows the peaks corresponding to the excited states and to the triplet states—those in the middle of the figure. From the left-hand side the first peak corresponds to the transmission through the one-electron ground state with charge fluctuations between the states with zero and one electron, for which the energy difference is $\Delta E_{01} = E_0 - E_1 = +|t|$ (for the eigenvalues see table A.1 in the appendix). The second conductance peak is at $\Delta E_{1\rm s} = E_1 - E_{\rm s} = -|t| - (U - \Delta)/2$, and corresponds to the charge fluctuations between the one-electron state and the two-electron ground state (the singlet state with E_+). Symmetrically on the right-hand side of the figure there are the conductance

peaks corresponding to the fluctuations between the three-electron and the four-electron states at $\Delta E_{34} = E_3 - E_4 = -|t| - U$, as well as between the two-electron and the three-electron states at $\Delta E_{s3} = E_- - E_3 = +|t| - (U + \Delta)/2$. The amplitude of these peaks is higher than those corresponding to the excited states. The positions of the transmission peaks through the triplet states are at $\Delta E_{1t} = E_1 - E_t = -|t|$ and $\Delta E_{t3} = E_t - E_3 = |t| - U$.

Let us now consider the low temperature limit and the problem of influence of the many particle states on the electronic transport. Our procedure used in the calculations of the conductance neglects the spin fluctuations and the Kondo effect. The conductance is sensitive to changes in the density of states (DOS) close to the Fermi energy. In the low temperature limit, below the Kondo temperature, the DOS shows a Abrikosov–Suhl peak [26, 14], strongly depending on temperature. Our procedure neglects this peak, and it gives reliable results at high temperatures. However, the correlation functions are calculated as integrals and the whole DOS below the Fermi energy contributes to these quantities. The correlation functions are, therefore, less sensitive to the DOS changes close to the Fermi energy than the conductance. One can expect that our computational procedure also gives reliable results for the correlation functions in the low temperature limit. We want to discuss the problem of screening of the magnetic moment by conduction electrons in the 2QD system. The case of the centre of the electronic structure, corresponding to two electrons present at the 2QD, is especially interesting, because one can study the transition from the molecular to the atomic state when the interdot coupling is changed. One could observe an evolution of the conductance with a change of the spin configuration. According to our best knowledge the effect has not been studied experimentally in two quantum dots connected in series. For low interdot couplings ($t \ll \Gamma_\alpha$) the spins in 2QD are decoupled, therefore, one expects the double Kondo resonance. The effect can be observed in source–drain measurements as a zero-voltage peak in the differential conductance, which is a characteristic feature of the Kondo resonance. In the strong coupling regime ($t \gg \Gamma_\alpha$) the spins are antiferromagnetically coupled and the Kondo effect is absent. A similar situation was predicted theoretically by Izumida *et al* [16], and Hofstetter and Schoeller [27] for a multilevel quantum dot, which was just recently verified experimentally by Kogan *et al* [28].

4. Summary

In the paper we have considered the effects of charge fluctuations in electronic transport through two mesoscopic devices: the quantum point contact (QPC) and the system of two quantum dots (2QD) connected in series. The studies of the QPC are based on the assumption of a specific electronic energy structure with a resonant level below the electronic sub-band. We have shown that the charge fluctuations on the resonant state lead to the dynamical Coulomb blockade effect, which reduces the conductance. The plateau appears at $\mathcal{G}_0 \approx 2/3 \times 2e^2/h$, which evolves to $1/2 \times 2e^2/h$ in a high magnetic field. For a non-equilibrium situation, the plateau position is shifted toward $0.4 \times 2e^2/h$ and $0.8 \times 2e^2/h$, depending on the relative position of the resonant state with respect to the Fermi energy at zero bias. The model is simplified, but it shows many similarities with experimental characteristics.

Our calculation method can be extended into the low temperature limit including spin correlations, which lead to the Kondo effect and an increase of the conductance plateau to $2e^2/h$. It can be performed within the EOM method using a higher order decoupling procedure for many body Green functions [29]. We believe that the model can also be generalized and applied to quantum wires, in which 0.7 structures were observed as well [30]. For this case a quantitative analysis of a charge accumulation and Coulomb interactions is needed. Preliminary studies of a long QPC show a large charge accumulation and a large value of the intra-level Coulomb integral for two electrons with opposite spins at the lowest resonant level. It suggests

an anomalous conductance plateau in a narrow energy range, in the range much narrower than in a short QPC.

For the 2DQ we studied the evolution of the energy dependence of the conductance and the spin correlation functions with changing of interdot hopping parameter, which can be directly controlled in experiments. For a weak-to-intermediate coupling between the 2QD and the leads, the energy dependence of the conductance exhibits a multi-peak structure with the positions of the peaks corresponding to the intradimer electron transitions. In the range of the intermediate 2QD–lead coupling, apart from the dominating peaks corresponding to the transitions between the degenerate ground states of the 2QD, the secondary peaks corresponding to transitions to the excited triplet states can also be seen. A contribution from the triplet states leads to the enhancement of the conductance near the centre of the energy structure and is particularly well seen in the region of intermediate interdot hopping. Here, the decrease in the absolute value of the spin–spin correlation function, indicating the decrease of antiferromagnetic coupling between the dots, is accompanied by a conductance rise. From the analysis of the interdot coupling dependence of the spin–spin correlations, we speculate that the transition from the molecular to the two-Kondo state should also be seen in experiments, in the grey scale conductance plots, for even numbers of electrons in 2QD. In low temperatures the zero-bias peak should be seen in the two-Kondo state (in a weak coupling regime), but it should disappear for the molecular state (for a strong coupling).

In the 2QD studies we have applied the Hubbard operator method, which takes into account exactly all electron and spin correlations within the strongly interacting central regions, even if some higher order correlations with electrons from the leads are neglected. The applied approximations reduce to the exact results in the case of vanishing interactions as well as for the very small coupling to the leads. The approach can be naturally extended to the larger systems provided that their energy structures are obtained.

Acknowledgments

We acknowledge fruitful discussions with Anton Ramsak and John Jefferson, and technical assistance in calculations by Michal Bek. The work was supported by the project RTNNANO contract No MRTN-CT-2003-504574 and in part by the Ministry of Science and Higher Education (Poland) within a research project.

Appendix. Charge fluctuations in ensemble of dimers

Here, we consider an ensemble of dimers including charge fluctuations. The solution of the dimer problem described by the Hubbard model has been previously given by Harris and Lange [31]. The eigenenergies and eigenvalues are presented in table A.1. The average of the quantity $\mathcal{O}$ is given by

$$\langle \mathcal{O} \rangle = \frac{1}{Z} \sum_{\lambda} \langle \lambda | \mathcal{O} | \lambda \rangle \mathrm{e}^{-\beta(E_\lambda - \mu N_\lambda)}, \tag{23}$$

where $\{E_\lambda, \lambda\}$ is the set of eigenenergies and eigenstates, the partition function $Z = \sum_\lambda \mathrm{e}^{-\beta(E_\lambda - \mu N_\lambda)}$, $\beta = 1/k_\mathrm{B}T$, μ is the chemical potential and N_λ is the number of electrons at the λ-state. The spin correlation functions can be written as

$$\langle \mathbf{S}_{\mathrm{tot}}^2 \rangle = \langle \mathbf{S}_1^2 \rangle + 2\langle \mathbf{S}_1 \cdot \mathbf{S}_2 \rangle + \langle \mathbf{S}_2^2 \rangle, \tag{24}$$

$$\langle \mathbf{S}_1^2 \rangle = \tfrac{3}{2}(\langle n_{1\uparrow} \rangle - \langle n_{1\uparrow} n_{1\downarrow} \rangle), \tag{25}$$

Table A.1. States and eigenvalues of the Hubbard dimer. Below we used $\epsilon_1 = \epsilon_2 = \epsilon$, $\alpha_\pm = 2|t|/\sqrt{2(4t^2 + E_\pm^2)}$, $\beta_\pm = E_\pm/\sqrt{2(4t^2 + E_\pm^2)}$, and $E_\pm = (U \pm \Delta)/2$, $\Delta = \sqrt{16t^2 + U^2}$.

Number of electrons	State	Eigenvalue
1	$1/\sqrt{2}(d^\dagger_{1\sigma} \pm d^\dagger_{2\sigma})\|\text{vac}\rangle$	$\epsilon \pm t$
2	$d^\dagger_{1\uparrow}d^\dagger_{2\uparrow}\|\text{vac}\rangle$ $1/\sqrt{2}(d^\dagger_{1\uparrow}d^\dagger_{2\downarrow} + d^\dagger_{1\downarrow}d^\dagger_{2\uparrow})\|\text{vac}\rangle$ $d^\dagger_{1\downarrow}d^\dagger_{2\downarrow}\|\text{vac}\rangle$	2ϵ
	$[\alpha_\pm(d^\dagger_{1\uparrow}d^\dagger_{2\downarrow} - d^\dagger_{1\downarrow}d^\dagger_{2\uparrow}) + \beta_\pm(d^\dagger_{1\uparrow}d^\dagger_{1\downarrow} + d^\dagger_{2\uparrow}d^\dagger_{2\downarrow})]\|\text{vac}\rangle$	$2\epsilon + E_\pm$
	$1/\sqrt{2}(d^\dagger_{1\uparrow}d^\dagger_{1\downarrow} - d^\dagger_{2\uparrow}d^\dagger_{2\downarrow})\|\text{vac}\rangle$	$2\epsilon + U$
3	$1/\sqrt{2}(d^\dagger_{1\sigma}d^\dagger_{2\uparrow}d^\dagger_{2\downarrow} \pm d^\dagger_{2,\sigma}d^\dagger_{1\uparrow}d^\dagger_{1\downarrow})\|\text{vac}\rangle$	$3\epsilon + U \pm t$
4	$d^\dagger_{1\uparrow}d^\dagger_{1\downarrow}d^\dagger_{2\uparrow}d^\dagger_{2\downarrow}\|\text{vac}\rangle$	$4\epsilon + 2U$

$$\langle \mathbf{S}_1 \cdot \mathbf{S}_2 \rangle = \tfrac{3}{2}(\langle n_{1\uparrow} n_{2\uparrow} \rangle - \langle n_{1\uparrow} n_{2\downarrow} \rangle). \tag{26}$$

Using table A.1 one can derive

$$\langle n_{1\uparrow} n_{1\downarrow} \rangle = [\mathrm{e}^{2\beta\mu}(\beta_+^2 \mathrm{e}^{-\beta E_+} + \beta_-^2 \mathrm{e}^{-\beta E_-} + 1/2\mathrm{e}^{-\beta U}) + 2\mathrm{e}^{\beta(3\mu - U)} \cosh(\beta t) + \mathrm{e}^{\beta(4\mu - 2U)}]/Z, \tag{27}$$

$$\langle n_{1\uparrow} n_{2\uparrow} \rangle = [\mathrm{e}^{2\beta\mu} + 2\mathrm{e}^{\beta(3\mu - U)} \cosh(\beta t) + \mathrm{e}^{\beta(4\mu - 2U)}]/Z, \tag{28}$$

$$\langle n_{1\uparrow} n_{2\downarrow} \rangle = [\mathrm{e}^{2\beta\mu}(1/2 + \alpha_+^2 \mathrm{e}^{-\beta E_+} + \alpha_-^2 \mathrm{e}^{-\beta E_-}) + 2\mathrm{e}^{\beta(3\mu - U)} \cosh(\beta t) + \mathrm{e}^{\beta(4\mu - 2U)}]/Z, \tag{29}$$

$$Z = 1 + 4[\mathrm{e}^{\beta\mu} + \mathrm{e}^{\beta(3\mu - U)}] \cosh(\beta t) + \mathrm{e}^{2\beta\mu}[3 + \mathrm{e}^{-\beta U} + 2\mathrm{e}^{-\beta U/2} \cosh(\beta\Delta/2)] + \mathrm{e}^{\beta(4\mu - 2U)}. \tag{30}$$

The chemical potential should be determined from the condition $n = (1/\beta)(\partial \ln Z/\partial\mu)$ for the fixed number of electrons n in the system. For the half-filling $\langle n_{1\uparrow} \rangle = 1/2$, the chemical potential $\mu = U/2$, independent of temperature.

References

[1] Thomas K J, Nicholls J T, Simmons M Y, Pepper M, Mace D R and Ritchie D A 1996 *Phys. Rev. Lett.* **77** 135

[2] Thomas K J, Nicholls J T, Appleyard N J, Simmons M Y, Pepper M, Mace D R, Tribe W R and Ritchie D A 1998 *Phys. Rev.* B **58** 4846

[3] Kristensen A, Lindelof P E, Jensen J B, Zaffalon M, Hollingbery J, Pedersen S W, Nygard J, Bruus H, Reimann S M, Srensen C B, Michel M and Forchel A 1998 *Physica* B **249–251** 180

[4] Kristensen A, Bruus H, Hansen A E, Jensen J B, Lindelof P E, Marckmann C J, Nygard J, Srensen S B, Beuscher F, Forchel A and Michel M 2000 *Phys. Rev.* B **62** 10950

[5] Devoret M H, Esteve D, Grabert H, Ingold G L, Pothier H and Urbina C 1990 *Phys. Rev. Lett.* **64** 1824
Levy Yeyati A, Martin-Rodero A, Esteve D and Urbina C 2001 *Phys. Rev. Lett.* **87** 046802
Agraït N, Levi Yeyati A and van Ruitenbeek J M 2003 *Phys. Rep.* **377** 81 and references therein

[6] Wang C K and Berggren K F 1998 *Phys. Rev.* B **57** 4552
Starikov A A, Yakimenko I I and Berggren K F 2003 *Phys. Rev.* B **67** 235319
Bruus H, Cheianov V V and Flensberg K 2001 *Physica* E **110** 97
Spivak B and Zhou F 2000 *Phys. Rev.* B **61** 16730
Hirose K, Meir Y and Wingreen N S 2003 *Phys. Rev. Lett.* **90** 026804
Reimann S M, Koskinen M and Manninen M 1999 *Phys. Rev.* B **59** 1613

[7] Rejec T, Ramsak A and Jefferson J H 2000 *Phys. Rev.* B **62** 12985
Rejec T, Ramsak A and Jefferson J H 2003 *Phys. Rev.* B **67** 075311
[8] Seelig G and Matveev K A 2003 *Phys. Rev. Lett.* **90** 176804
[9] Meir Y, Hirose K and Wingreen N S 2002 *Phys. Rev. Lett.* **89** 196802
[10] Rokhinson L P, Pfeiffer L N and West K W 2006 *Phys. Rev. Lett.* **96** 156602
[11] Cronenwett S M, Lynch H J, Goldhaber-Gordon D, Kouwenhoven L P, Marcus C M, Hirose K, Wingreen N S and Umansky V 2002 *Phys. Rev. Lett.* **88** 226805
Cronenwett S M 2001 *PhD Thesis* Stanford University
[12] Blick R H, Pfannkuche D, Haug R J, von Klitzing K and Eberl K 1998 *Phys. Rev. Lett.* **80** 4032
Holleitner A W, Decker C R, Qin H, Eberl K and Blick R H 2001 *Phys. Rev. Lett.* **87** 256802
Holleitner A W, Blick R H, Huttel A K, Eberl K and Kotthaus J P 2002 *Science* **297** 70
Rogge M C, Fuhner C, Keyser U F, Haug R J, Bichler M, Abstreitere G and Wegscheider W 2003 *Appl. Phys. Lett.* **83** 1163
[13] Jeong H, Chang A M and Melloch M R 2001 *Science* **293** 2221
Qin H, Holleitner A W, Eberl K and Blick R H 2001 *Phys. Rev.* B **64** 241302
Pioro-Ladriere M, Ciorga M, Lapointe J, Zawadzki P, Korkusiński M, Hawrylak P and Sachrajda A S 2003 *Phys. Rev. Lett.* **91** 026803
Hayashi T, Fujisawa T, Cheong H D, Jeong Y H and Hirayama Y 2003 *Phys. Rev. Lett.* **91** 226804
Blick R H, Huttel A K, Holleitner A W, Hohberger E M, Qin H, Kirschbauma J, Weber J, Wegscheider W, Bichler M, Eberl K and Kotthaus J P 2003 *Physica* E **16** 76
Pustilnik, M, Glazman L I, Cobden D H and Kouwenhoven L P 2001 *Lecture Notes Phys.* **579** 3
Petta J R, Johnson A C, Marcus C M, Hanson M P and Gossard A C 2004 *Phys. Rev. Lett.* **93** 186802
van der Wiel W G, De Franceschi S, Elzerman J M, Fujisawa T, Tarucha S and Kouwenhoven L P 2003 *Rev. Mod. Phys.* **75** 1
[14] Georges A and Meir Y 1999 *Phys. Rev. Lett.* **82** 3508
Kouwenhoven L and Glazman L I 2001 *Phys. World* **14** 33 and references therein
[15] Pustilnik M, Avishai Y and Kikoin K 2000 *Phys. Rev. Lett.* **84** 1756
Pustilnik M and Glazman L I 2000 *Phys. Rev. Lett.* **85** 2993
Pustilnik M and Glazman L I 2001 *Phys. Rev. Lett.* **87** 216601
Pustilnik M and Glazman L I 2001 *Phys. Rev.* B **64** 045328
[16] Izumida W, Sakai O and Tarucha S 2001 *Phys. Rev. Lett.* **87** 216803
Sakai O and Izumida W 2003 *Physica* B **328** 125
[17] Kawamura K and Aono T 1997 *Japan. J. Appl. Phys.* **36** 3951
Aono T, Eto M and Kawamura K 1998 *J. Phys. Soc. Japan* **67** 1860
Aono T, Eto M and Kawamura K 1999 *Japan. J. Appl. Phys.* **38** 315
Aono T and Eto M 2001 *Phys. Rev.* B **63** 125327
Ziegler R, Bruder C and Schoeller H 2000 *Phys. Rev.* B **62** 1961
Aguado R and Langreth D C 2000 *Phys. Rev. Lett.* **85** 1946
Lopez R, Augado R and Platero G 2002 *Phys. Rev. Lett.* **89** 136802
Orellana P A, Lara G A and Anda E V 2002 *Phys. Rev.* B **65** 155317
Aguado R and Langreth D C 2003 *Phys. Rev.* B **67** 245307
[18] Haug H and Jauho A P 1998 *Quantum Kinetics in Transport and Optics of Semiconductors* (Berlin: Springer)
[19] Bulka B R and Kostyrko T 2004 *Phys. Rev.* B **70** 205333
[20] Meir Y, Wingreen N S and Lee P A 1991 *Phys. Rev. Lett.* **66** 3048
[21] Kostyrko T and Bulka B R 2005 *Phys. Rev.* B **71** 235306
[22] Pals P and MacKinnon A 1996 *J. Phys.: Condens. Matter* **8** 5401
[23] You J Q and Zheng H Z 1999 *Phys. Rev.* B **60** 13314
[24] Hubbard J 1964 *Proc. R. Soc.* A **277** 237
[25] Niu C, Lin D L and Lin T H 1999 *J. Phys.: Condens. Matter* **11** 1511
[26] Hewson A C 1993 *The Kondo Problem to Heavy Fermions* (Cambridge: Cambridge University Press)
[27] Hofstetter W and Schoeller H 2002 *Phys. Rev. Lett.* **88** 016803
[28] Kogan A, Granger G, Kastner M A, Goldhaber-Gordon D and Shtrikman H 2003 *Phys. Rev.* B **67** 113309
[29] Lacroix C 1981 *J. Phys. F: Met. Phys.* **11** 2389
see also Bulka B R and Stefanski P 2001 *Phys. Rev. Lett.* **86** 5128
[30] Thomas K J, Nicholls J T, Pepper M, Tribe W R, Simmons M Y and Ritchie D A 2000 *Phys. Rev.* B **61** 13365
Reilly D J, Facer G R, Dzurak A S, Kane B E, Clark R G, Stiles P J, Clark R G, Hamilton A R, O'Brien J L and Lumpkin N E 2001 *Phys. Rev.* B **63** 121311
de Picciotto R, Pfeiffer L, Baldwin K and West K 2004 *Phys. Rev. Lett.* **92** 036805

de Picciotto R, Pfeiffer L N, Baldwin K W and West K W 2005 *Phys. Rev.* B **72** 033319
Giannetta R W, Olheiser T A, Hannan M, Adesida I and Melloch M R 2005 *Physica* E **27** 270
Danneau R, Clarke W R, Klochan O, Micolich A P, Hamilton A R, Simmons M Y, Pepper M and Ritchie D A 2006 *Appl. Phys. Lett.* **88** 012107
[31] Harris A B and Lange R V 1967 *Phys. Rev.* **157** 295